第22卷 第5期 2000年 9月
岩 土 工 程 学 报
Chinese Journal of Geotechnical Engineering
Vol. 22 No. 5 Sept., 2000

Microscopic shear mechanism of granular materials in simple shear by DEM
用离散单元法分析单剪试验中粒状体的剪切机理

Liu Sihong (刘斯宏) *Lu Tinghao* (卢廷浩)
(Nagoya Institute of Technology, Japan) (Hohai University, Nanjing, 210098, China)

Abstract By using a special two-dimensional simple shear test apparatus with rigid lateral platens, simple shear tests are carried out on an assembly of aluminum rods, one of which is then simulated by distinct element method (DEM). The simulation results by DEM agree well with the test results. Based on the simulation results, the shear mechanism of granular materials in simple shear test, such as the frequency distribution and the variation of contact angles of particles along the mobilized plane, is studied.

Key words distinct element method, granular material, microscopic, simple shear test

Liu Sihong born in 1964, Dr., researcher of Nagoya Institute of Technology

文 摘 用铝棒堆积体作为二维粒状体的模型材料进行单剪试验,然后对其用离散单元法进行数值模拟,对于宏观应力应变关系,两者结果基本吻合。基于数据模拟结果,对粒状体的剪切机理,例如滑动面上粒子接点角的分布及变化规律,进行了微观分析。

关键词 离散单元法,粒状体,微观,单剪试验
中图法分类号 TU 411.7 **文献标识码** A **文章编号** 1000-4548(2000)05-0608-04

1 Introduction*

Macroscopic mechanical features of granular materials are closely related to the behavior of individual particles. So far, many researchers have studied on macroscopic responses of granular materials under shear from a microscopic viewpoint. For example, Oda and Konishi(1974) carried out simple shear tests on assemblies of photoelastic rods and found that the frequency distribution of contact orientations of granular materials tends to concentrate around the major principal stress axis. Matsuoka(1974) performed direct box shear tests on assemblies of aluminum and photoelastic rods and derived a relationship between shear-normal stress ratio and normal-shear strain increment ratio on the mobilized plane. Recently, distinct element method(DEM), which was proposed by Cundall and Strack (1979), has been widely used to study micromechanics of granular materials (e.g. Wang and Xing, 1991, Yamamoto et al. 1994, 1995), because it has a great merit that displacements, contact forces, contact orientations of particles and so on can be calculated easily and exactly. In this paper, a simple shear test on an assembly of aluminum rods is simulated by DEM, and based on the simulation results, the shear mechanism of granular materials is studied from a microscopic viewpoint.

2 Simple shear test on assembly of aluminum rods

In this study, a special two-dimensional simple shear test apparatus was built up. Fig. 1(a) shows its picture and Fig. 1(b) the schematic view of this apparatus. In this apparatus, the lateral walls are two rigid platens, which are connected to both the base platen and a rigid bar at the upper backside with two hinges, respectively. The geometrical configuration of it keeps the same rotation angle of both the left and the right lateral walls. The upper loading platen on the specimen is pulled horizontally with a rope while a constant dead load is applied on the specimen, thus resulting in an inclination of the two lateral walls and production of shear

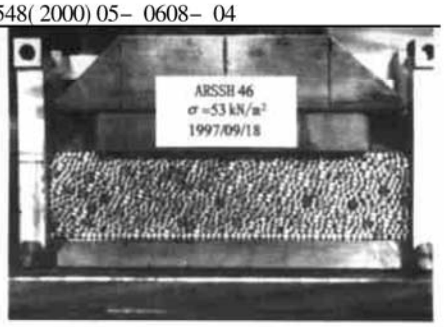

(a)

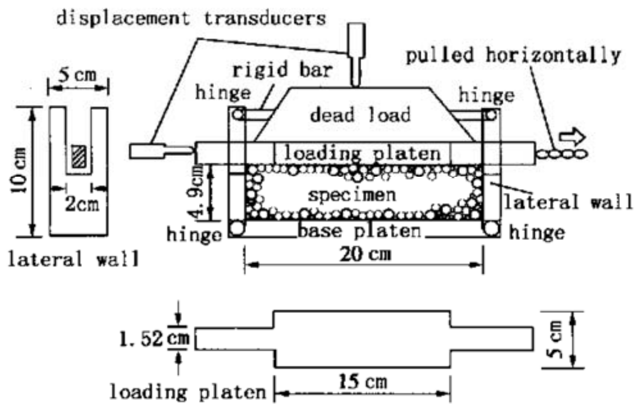

(b)

Fig. 1 Two-dimensional simple shear test apparatus

strains in the specimen. The specimen consists of an assembly of aluminum rods with 3 mm and 5mm in diameters, 50 mm in length and 3∶2 in mixing ratio by weight. A layer of the same aluminum rods as the specimen is pasted on both the downward surface of the upper loading platen and the upward surface of the base platen, which is indicated in Fig. 1(b) by bold circles, to make them have sufficient frictions. The dimensions and the initial void ratio of the specimen are 20 cm × 4.9 cm (width × height) and 0.201, respectively. The normal (vertical) stress, σ_N, which is

* Received March 15, 2000

applied by dead load, is 52 kPa. Fig. 2 gives the test results with respect to the relationships among shear - normal stress ratio τ/σ_N, shear strain γ and normal (vertical) strain ε_N, represented by broken plots (○).

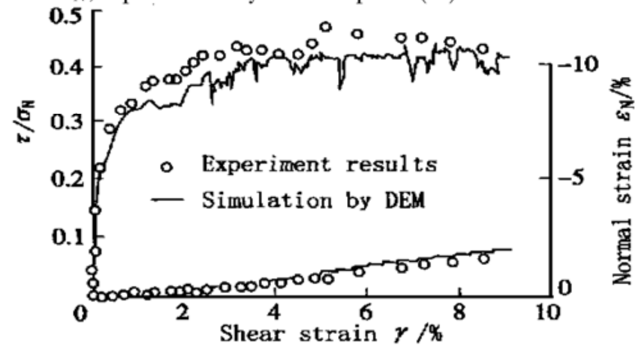

Fig. 2 Comparison between experiment results and simulation results by DEM

3 Simulation of simple shear test by DEM

In DEM, the granular material is envisaged to be composed of rigid discs connected to each other at the contacts by elastic springs and viscous dashpots, as modeled in Fig. 3. In Fig. 3, a divider is modeling that no contact forces exist between two particles if they separate each other; and a slider is modeling that the Coulomb- type friction law is incorporated for checking the shear force between two particles along the tangential direction.

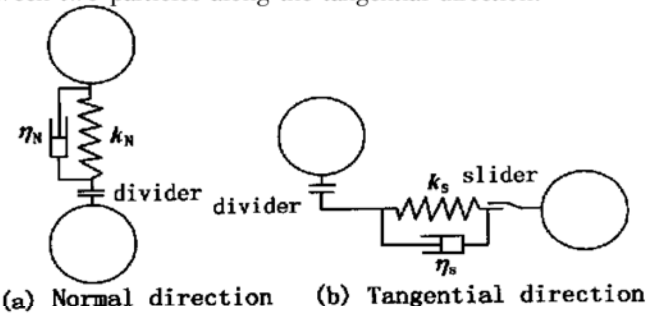

Fig. 3 Contact models of two rigid discs in DEM

Fig. 4 shows the initial particle arrangement used in DEM simulation, which was digitized from the picture as shown in Fig. 1(a). Table 1 gives the input parameters for DEM simulation. The stiffness(k_n, k_s) and damping η_N, η_s in Table 1 are determined from the contact theory of two elastic discs and the interparticle friction angle φ_μ between aluminum rods from a simple frictional test(Matsuoka and Yamamoto, 1994).

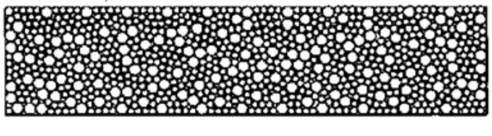

Fig. 4 Arrangement of initial particles used in DEM simulation

The DEM simulation results with respect to macroscopic stress- strain relations are shown in Fig. 2 by solid lines together with the experimental results. As seen from Fig. 2, the numerical results by DEM agree well with the experimental results, indicating the effectiveness and accuracy of the DEM simulation.

Since the geometrical configuration of this simple shear apparatus ensures the same inclination of the left and the right lateral rigid platens, the potential mobilized planes in the specimen may be assumed to be horizontal. This assumption can be confirmed through the next investigation of the displacement distributions within the specimen and the orientations of the principal stresses calculated from contact forces of particles. Fig. 5 gives the distribution of the total displacements within the specimen accumulated from the beginning of shearing to the peak shear strength, where the solid inclined lines correspond to the inclination of the lateral rigid platens(either the left or the right) and the plots represent the results of the numerical simulation. The total displacements are averaged at every 5cm wide span of the specimen along the specimen height. It can be seen from Fig. 5 that the total displacements within the specimen are almost the same as those of the lateral platens at the same level, namely, the shear strains through the specimen are reasonably uniform. Fig. 6 shows the orientations of principal stress at peak shear strength calculated from the contact forces by using the formula

$$\sigma_{ij} = \sum_R l_i F_j \Big/ V \quad (1)$$

(Christoffersen et al., 1981), where R is the calculating domain, V is the volume of the domain, l_i is the length of vectors connecting the centers of contacting particles, and F_j is the contact force. In Fig. 6, the frequency distribution of contact angles is also illustrated. It can be seen from Fig. 6 that, at peak shear strength, the major principal stress calculated by Eq. (1) is inclined to the horizontal plane at an angle of about 33°. On the other hand, as the internal friction angle, φ, at peak shear strength is equal to 22.8°($\tan^{-1}(\tau/\sigma_N) = \tan^{-1}0.42$), thus the angle between the major principal stress and the mobilized plane is

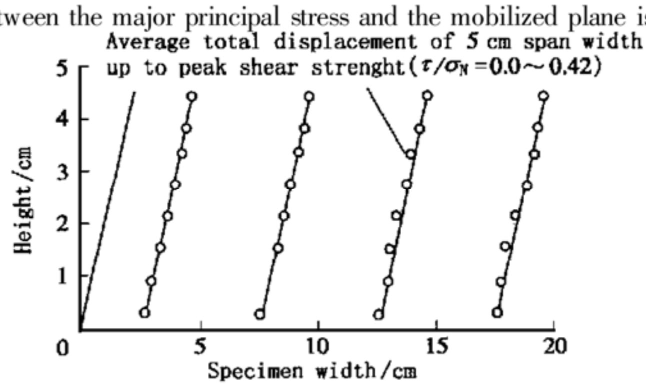

Fig. 5 Distribution of total displacements along specimen height, averaged at every 5cm width

Table 1 Input parameters for numerical simulation by DEM

the granular material	k_N /(N•m⁻¹•m⁻¹)	k_S /(N•m⁻¹•m⁻¹)	η_N /(N•s•m⁻¹•m⁻¹)	η_S /(N•s•m⁻¹•m⁻¹)	φ_μ /(°)	ρ /(kg•m⁻³)	Δt /s
particle- particle	9.0×10^{9}	3.0×10^{8}	7.9×10^{4}	1.4×10^{4}	16	2700	2×10^{-7}
particle- platen	1.8×10^{10}	6.0×10^{8}	1.1×10^{5}	2.0×10^{4}	16	2700	2×10^{-7}

equal to $(\pi/4 - \varphi/2) = 33.6°$, which agrees nearly with the angle calculated from the contact forces of particles. Next, we study the shear mechanism of granular materials in simple shear based on the assumption that the direction of the mobilized plane is horizontal.

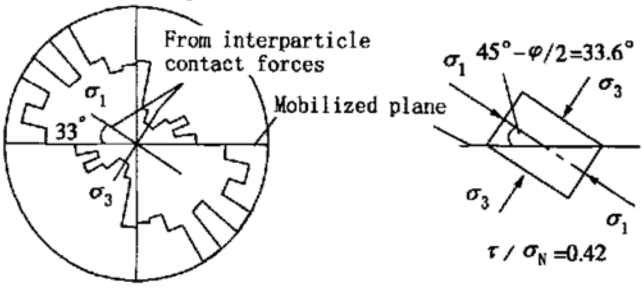

Fig. 6 Orientations of principal stresses at peak shear strength calculated from contact forces

4 Fabric change in granular materials during shear

Fig. 7 shows the frequency distribution of contact normal orientations $M(\alpha)$ during shear, where α is defined as the inclination angle of the contact normal to the mobilized plane (Fig. 8). As seen in Fig. 7, $M(\alpha)$ tend to concentrate toward a preferred direction which gradually rotates with the increase in the shear stress. This preferred direction of $M(\alpha)$ agrees nearly with the direction of the major principal stress, as reported by Oda et al. (1974). Fig. 9 shows the normalized frequency distribution of contact angles $N(\theta)/N_{\max}$ on the mobilized plane using the same data as Fig. 7, where θ is defined as the contact angle (Fig. 8). It is seen from Fig. 9 that, with the increase in shear stress, the distribution of $N(\theta)$ shifts to the right side, that is, the number of contacts on the mobilized plane increases in the positive zone of θ where the contacting particles are effective to resist shearing (Matsuoka, 1974). Essentially, the shift of $N(\theta)$ distribution on the mobilized plane to the positive zone of θ is the same as the concentration of $M(\alpha)$ in the major principal stress direction. Then, we consider the reason why $M(\alpha)$ concentrates around the major principal stress direction and $N(\theta)$ is shifted one-sided to the positive zone of θ. Fig. 10(a) shows the frequency distribution of contact normals which have newly been generated during shear, $M_g(\alpha)$, and Fig. 10(b) the frequency distribution of contact normals which have disappeared during shear, $M_d(\alpha)$, from the shear beginning ($\tau/\sigma_N = 0$) to the peak shear strength ($\tau/\sigma_N = 0.42$). The contact corresponding to $M_g(\alpha)$ and $M_d(\alpha)$ is called an "generated contact" and "disappearing contact" (cf. Fig. 11), respectively (Matsuoka and Takeda, 1980). It is interesting to find from Fig. 10 that the "generated contact" normals concentrate in the major principal stress direction, while the "disappearing contact" normals concentrate in the minor principal stress direction. This results in the concentration of contact normals in the major principal stress direction as shown in Fig. 7. Furthermore, Fig. 12 shows the "generated contact" $N_g(\theta)$ and the "disappearing contact" $N_d(\theta)$ on the mobilized plane when τ/σ_N increases from 0 to 0.42. Similarly, it is interesting to notice that $N_g(\theta)$ concentrates in the positive zone of θ, while $N_d(\theta)$ concentrates in the negative zone of θ. This is the reason why the distribution of $N(\theta)$ on the mobilized plane shifts to the positive zone of θ where it is effective to resist shearing, as shown in Fig. 9.

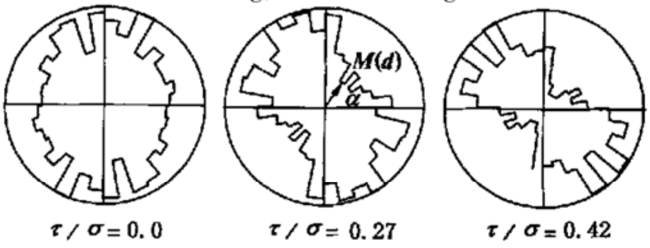

Fig. 7 Frequency distribution of contact normals $M(\alpha)$ during shear

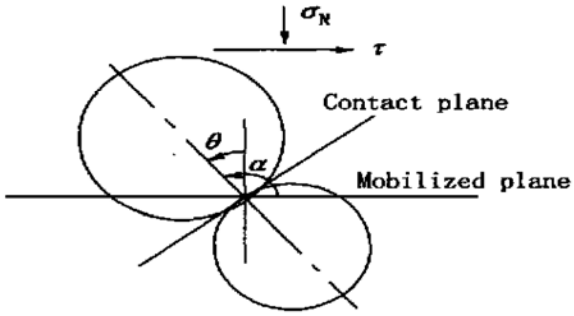

Fig. 8 Definition of contact angle θ and contact normal orientation α

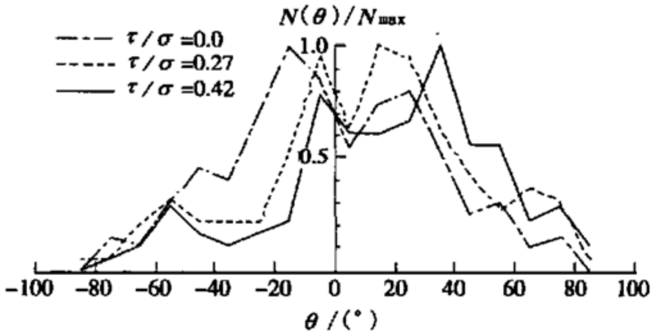

Fig. 9 Variation of contact angles on the mobilization plane during shear

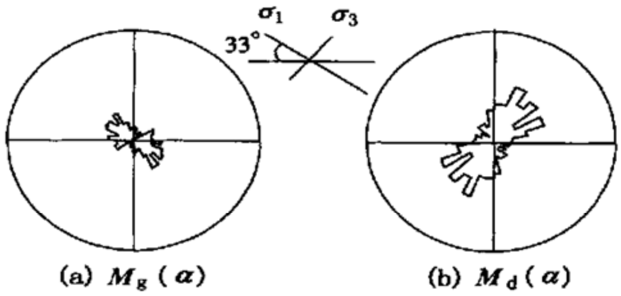

Fig. 10 Frequency distribution of contact normals

5 Distribution of change in contact angles on mobilized plane

Fig. 13 shows the distribution of the change in contact angles ξ for such contacts that keep in contact (cf. Fig. 11) during the increase of τ/σ_N from 0 to 0.42 along the mobilized plane, where ξ is positive when the contact angle increases in the direction of the shear stress. The curve line in Fig. 13 is drawn by fitting the plots on the basis of the shear-normal stress ratio $\tau(\theta)/\sigma_N(\theta)$ on the contact

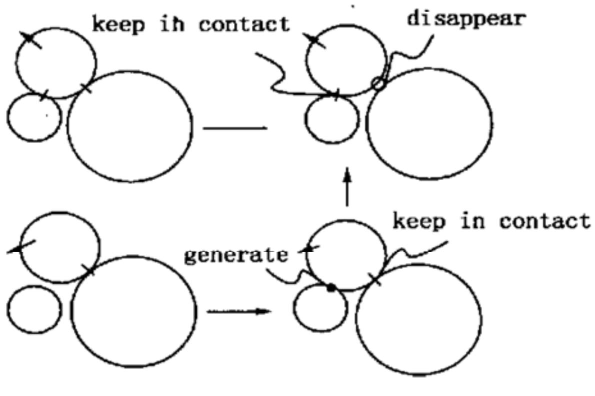

Fig. 11 Mechanism of disappearing contact and generated contact

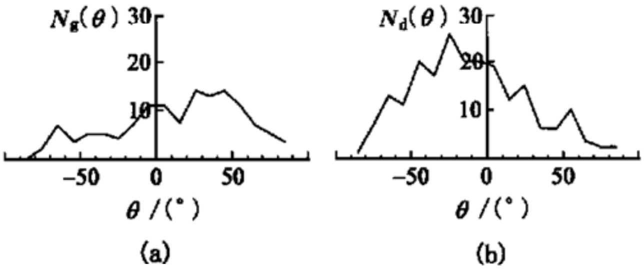

Fig. 12 Frequency distribution of contact angles on mobilized plane

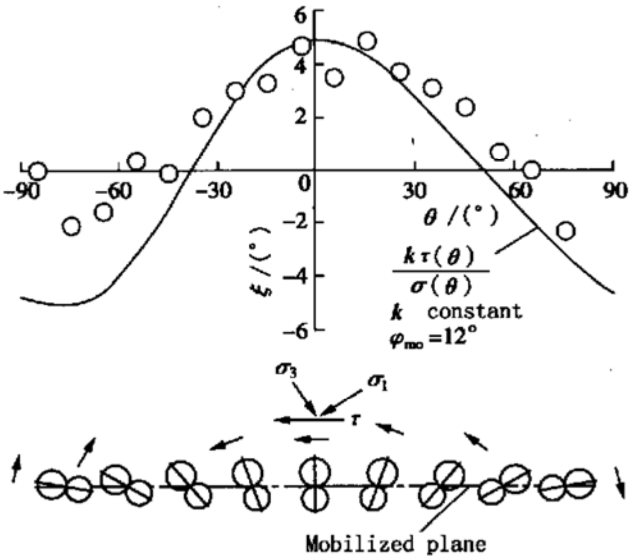

Fig. 13 Distribution of change in contact angles on mobilized plane

plane, which is expressed as

$$\frac{\tau(\theta)}{\sigma_N(\theta)} = \frac{\sin\varphi_{mo}\cos(2\theta - \varphi_{mo})}{1 + \sin\varphi_{mo}\sin(2\theta - \varphi_{mo})} \qquad (2)$$

It is seen from Fig. 13 that the distribution of the change in contact angles ξ along the mobilized plane is nearly proportional to the shear - normal stress ratio $\tau(\theta)/\sigma_N(\theta)$ on the contact plane. That is to say, the frictional law on the contact plane rules the movements of the particles on the mobilized plane. This is similar to the finding by Yamamoto et al. (1994, 1995) who simulated a biaxial compression test on an assembly of aluminum rods by DEM. The lower of Fig. 13 shows how the particles along the mobilized plane move (or rotate) corresponding to the contact angle θ. From that, it is understandable that ξ_{max} takes place when the contact plane coincides with the mobilized plane ($\theta = 0$), and $\xi = 0$ when the contact plane is parallel to the principal stresses (σ_1 or σ_3). Furthermore, it is interesting to notice that the particles along the mobilized plane tend to move (or rotate) to the stable plane along the direction of minor principal stress σ_3.

6 Concluding remarks

In this paper, a simple shear test on an assembly of aluminum rods is simulated by DEM. The simulation results with respect to the macroscopic stress- strain relations agree well with the experimental results. Based on the simulation results, the shear mechanism of granular materials in simple shear test is studied and the following two conclusions are obtained:

(1) With the increase in shear stress during shear, the contact normals tend to concentrate toward the major principal stress direction. The reason for this is that the "generated contact" normals concentrate around the major principal stress direction, while the "disappearing contact" normals concentrate around the minor principal stress direction, as shown in Fig. 10.

(2) The distribution of the change in interparticle contact angles is proportional to the macroscopic shear - normal stress ratio on the contact plane. That is to say, the frictional law on the contact plane rules the movements of the particles on the mobilized plane.

Acknowledgements

The authors wish to express their sincere gratitude to Prof. H. Matsuoka of Nagoya Institute of Technology for his guidance and invaluable support throughout this research. Great thanks are also extended to Dr. S. Yamamoto of Obayashi Corporation for his great help in DEM calculation.

References

1 Cundall P A, Strack O D L. A discrete numerical model for granular assemblies. Géotechnique, 1979, **29**(1): 47~ 65
2 Christoffersen J, Mehrabadi M M, Nemat- Nasser S. A micromechanical description of granular material behavior. J Appl Mech, 1981, **48**(2): 339~ 344
3 Matsuoka H. A microscopic study on shear mechanism of granular materials. Soils and Foundations, 1974, **14**(1): 29~ 43
4 Matsuoka H, Takeda K. A stress- strain relationship for granular materials derived from microscopic shear mechanism. Soils and Foundations, 1980, **20**(3): 45~ 58
5 Matsuoka H, Yamamoto S. A microscopic study on shear mechanism of granular materials by DEM. Journal of Geotechnical Engineering, JSCE, 1994, III- **26**(487): 167~ 175 (in Japanese)
6 Oda M, Konishi J. Microscopic deformation mechanism of granular material in simple shear. Soils and Foundations, 1974, **14**(4): 25~ 38
7 Oda M, Konishi J. Rotation of principal stresses in granular material during simple shear. Soils and Foundations, 1974, **14**(4): 39 ~ 53
8 王泳嘉, 邢纪波. 离散单元法及其在岩土力学中的应用. 东北工学院出版社, 1991
9 Yamamoto S, Matsuoka H. A relationship between fabric changes and shear strain of granular materials under shear. Journal of Geotechnical Engineering, JSCE, 1994, III- **29**(505): 219~ 228 (in Japanese)
10 Yamamoto S. Fundamental study on mechanical behavior of granular materials by [DEM. Eng Dr Thesis]. Nagoya Institute of Technology, 1995 (in Japanese)